EXCHANGE INTERPRETATION OF ANOMALOUS BACK ANGLE HEAVY ION ELASTIC SCATTERING

M. S. Zisman

Nuclear Science Division
Lawrence Berkeley Laboratory
University of California
Berkeley, California 94720

NOTICE
This report was prepared as an account of work sponsored by the United States Government. Neither the United States nor the United States Department of Energy, nor any of their employees, nor any of their contractors, subcontractors, or their employees, makes any warranty, express or implied, or assumes any legal liability or responsibility for the accuracy, completeness or usefulness of any information, apparatus, product or process disclosed, or represents that its use would not infringe privately owned rights.

I. INTRODUCTION

In the past few years a number of groups have been engaged in making careful studies of heavy ion elastic scattering.[1-4]) For example, data for the $^{16}O + ^{28}Si$ system have presently been obtained over the (laboratory) energy range of 33-215 MeV. While the results of a "global" optical model search yielded[1]) a strongly absorbing, energy independent potential (E18, see Table I) which fit the data rather well at both high and low energies, the intermediate energies, roughly $40 \leq E_{lab} \leq 60$ MeV, gave evidence for oscillations which were not reproduced by the optical model in any systematic fashion. In particular, it was found that any optical potential which produced suitable back angle oscillations at these intermediate energies invariably predicted that these oscillations would grow more pronounced at higher energies, at variance with the experimental data.

Very recently, additional information on this problem was provided by Braun-Munzinger et al.[5]), who extended the $^{16}O + ^{28}Si$ data at $E_{lab} = 55$ MeV back to 180° by bombarding Al_2O_3 targets with a ^{28}Si beam

DISTRIBUTION OF THIS DOCUMENT IS UNLIMITED

and measuring the recoil ^{16}O ions at forward angles. These data showed a highly structured angular distribution at c.m. angles beyond about 60°. In fact the angles beyond about 140° were described rather well by an angular distribution of the form $|P_{26}(\cos\theta)|^2$. Analysis of the data showed[5]) that the entire angular distribution can be fit by adding a Regge pole or shape resonance term directly to the "background" S-matrix as calculated with an optical potential such as E18.

This approach of using an S-matrix to which has been added a "resonance" term was also examined by Cramer et al.[6]) in an attempt to explain the other anomalous results at intermediate energies which have been obtained for the $^{16}O + {}^{28}Si$ system. They used a modified S-matrix of the form:

$$S_\ell = S_\ell^o \left[1 - ie^{2i\phi} \frac{\Gamma_e(1 - |S_\ell^o|^2)}{E_{c.m.} - E_{res}(\ell) + i\,\Gamma_t/2} \right]$$

where S_ℓ^o is the optical model background S-matrix, ϕ is the resonance mixing phase, Γ_e is the elastic reduced width of the resonance, Γ_t is the total width of the resonance, and $E_{res}(\ell)$ is the center of mass energy for the resonance with angular momentum ℓ. It was further suggested that the resonances formed a VMI rotational band in ^{44}Ti whose energies are given by

$$E_{res}(\ell) = 10.024 + 0.336\ [\ell(\ell + 1)]^{2/3} \quad ,$$

where the constants were obtained by individual fits at the various energies, using the same procedure as Braun-Munzinger et al.[5]) to obtain the pole ℓ values. Because the optical model grazing partial wave, ℓ_g,

has a different energy dependence, $E_{c.m.} \propto [\ell_g(\ell_g + 1)]$, than the VMI band, the resonances will eventually move away from ℓ_g and presumably become less apparent in the angular distributions.

As another approach to explaining the highly structured angular distribution obtained for back angle elastic scattering of $^{16}O + {}^{28}Si$ at $E_{lab} \approx 55$ MeV, we note that this sort of behavior is rather similar to the sort of effects one sees in the scattering of comparable mass heavy ions at intermediate energies.[7-9] In many such cases the data have been successfully fit by considering an exchange mechanism (generally called "elastic transfer"). Although the size of the transferred "cluster" in the $^{16}O + {}^{28}Si$ system is much larger than those generally considered by this mechanism, it seemed worthwhile (albeit somewhat implausible) to see what effects might be predicted by this model in the present case.

II. ELASTIC TRANSFER

The kinematics of the elastic transfer process are illustrated in Fig. 1. On the left-hand side, we have incoming particle A scattering from a composite particle $B = A' + x$, where A' is the "core" and x is a nucleon or nucleon cluster, through a scattering angle θ. On the right-hand side, we consider the transfer reaction $A + (A' + x) \rightarrow A' + (A + x)$ at angle $\pi - \theta$, where x is transferred from A' to A. Clearly, if cores A and A' are identical, both of these processes lead to the appearance of a particle A at θ and B at $\pi - \theta$ and are therefore indistinguishable. Quantum mechanically, such a process is one term in a fully anti-symmetrized DWBA calculation. Normally such exchange terms are small and are ignored, but in certain cases where the exchange of the cores is equivalent to

a simple transfer reaction, the exchange amplitude can be comparable to the direct term.[10]

In practice, calculations of this mechanism have been carried out by a variety of techniques ranging from the LCNO approximation[11] to no-recoil DWBA calculations[8] and, finally, to full finite-range DWBA calculations.[7,9] In the $^{16}O + ^{28}Si$ system, we are considering transfer of a relatively large cluster, ^{12}C. For this reason it is obvious that only a full finite range approach is appropriate. Therefore all calculations described here were carried out with the code LOLA.[12] The details of the calculation are outlined in Fig. 2. Briefly, one adds coherently the elastic scattering amplitude at θ (as obtained from an optical model calculation) to the transfer amplitude at angle $\pi - \theta$ (from the DWBA calculation) which is weighted by the appropriate spectroscopic factor, S. Note that in the case of elastic transfer the symmetry of the reaction means that only a <u>single</u> spectroscopic factor is required to describe the process. To be consistent with other authors,[7,13] I have included in the cross section expression an additional phase between the two amplitudes. This is often done in such calculations because other mechanisms, e.g., channel coupling effects, can in principle cause a phase shift in the interference pattern at different energies. However, for the calculations discussed here the phase $\alpha = 0$ expected for transfer of a spin-zero cluster between two 0^+ cores will be used. Although I know of no theoretical calculation of the spectroscopic factor for $^{28}Si \rightarrow ^{16}O + ^{12}C$, one can at least hope that the value resulting from elastic transfer calculations will be energy independent. Because of deficiencies with our choice

of a simple cluster wave function, as opposed to a more realistic microscopic calculation, and our lack of knowledge about the parameters of the Woods-Saxon well used to generate the bound state, it is in any case not obvious that one should expect to find that the "theoretical" value of S is the one which will reproduce the measured data.[14]

Given the assumption of an elastic transfer mechanism, we can make some general statements about the behavior we might expect without doing any calculations. For example, at "medium" energies, the elastic and transfer amplitudes will be comparable at intermediate angles, leading to a marked interference pattern. At "low" energies the elastic cross section becomes very large and the transfer cross section small. In this case the interference will tend to weaken at the intermediate angles and move backward in angle. Finally, at "high" energies, the reaction kinematics tend to push the cross sections for both the elastic and transfer processes to forward angles (that is, toward 0° for the elastic and toward 180° for the transfer.) In this situation the interference occurs in a region where the cross sections for both processes are very small and the two processes become, in effect, independent. Clearly these predictions are consistent with the behavior of the anomaly in $^{16}O + ^{28}Si$ elastic scattering described in Ref. 1

III. $^{16}O + ^{28}Si$ CALCULATIONS

A. 55 MeV Data

Figure 3 shows the data of Braun-Munzinger et al.[5] along with (separate) optical model and DWBA calculations for the elastic scattering and the $^{28}Si(^{16}O, ^{28}Si)$ reaction, respectively. [The spectroscopic

factor used in the figure and in all of the $^{16}O + ^{28}Si$ calculations discussed here is S = 0.3.] Optical parameter sets and bound state parameters are listed in Table I. We see from Fig. 3 that the back angle data are given quite well by the DWBA calculation. Furthermore, it is clear that in this case the interference between the two processes will be most pronounced in the angular region near 90°. The result of coherently adding the two processes is shown in Fig. 4. As expected, the forward and backward angular regions remain more or less unchanged, while the angular region between about 60 - 100° shows strong interference effects, in agreement with the experimental data.

The remaining discrepancy with the experimental data is that, in the angular region near 120° there is not predicted to be as much structure as was observed. In order to improve this aspect, in Fig. 5 a different optical potential set was tried which (probably because of reflection from the imaginary well) gives more elastic cross section at back angles. It is possible that this technique is mocking up some other effect, such as coupled channels,[14]) but I will not attempt to justify the choice of this optical potential (set O16C in Table I) other than by noting that, in this formalism, it is necessary to have some reasonable amplitude to "interfere" with. As can be seen, this change doesn't have a major effect on the DWBA part of the calculation. The results of the coherent addition are shown in Fig. 6. Now we find that the phase of the data is well-reproduced over the whole angular range, although the magnitude in the 100 - 150° region is still too large. This deficiency, which is common also to the calculations[5,6]) employing Regge poles, may be solved by a judicious

choice of optical parameters. Alternatively, it could be related to some sort of channel coupling effect.

B. Other Energies

Assuming this model is appropriate, we next ask what it predicts at higher and lower energies. Figure 7 shows the elastic transfer predictions for $^{16}O + ^{28}Si$ at 38 MeV compared with data from Ref. 2. We find, as expected, that the interference pattern gets weaker at middle angles and moves toward larger angles. The predicted oscillations near 90° are compatible with the existing data. Finally, in Fig. 8 we compare our model to existing $^{16}O + ^{28}Si$ data at 81 MeV. Again we find at least qualitative agreement, that is, the interference region is just beginning at about the place where the (structureless) data stop.

IV. $^{12}C + ^{28}Si$ CALCULATIONS

A. Rochester Data

Fighting the temptation to quit while ahead, we turn now to the recently measured back angle $^{12}C + ^{28}Si$ data from the Rochester group,[15]) which was discussed in an earlier talk. Here too it was found that a strongly absorbing potential such as H12 (see Table I), which was obtained in a global search of $^{12}C + ^{28}Si$ elastic scattering data[3]) covering a large energy range, did not produce enough structure in the back angle calculations. Therefore another optical potential, designated C12F in Table I, was chosen (in the spirit discussed above) which produced somewhat more favorable results.

The results of the calculations are compared with the data in Fig. 9. Unfortunately, with data at more than one energy our requirement of a constant spectroscopic factor for this "^{16}O transfer" reaction had to be relaxed. In fact it had to be modified in a strange way: Of the nine measured angular distributions, the four energies on the left side of Fig. 9 have $\sigma/\sigma_R \sim 10^{-2}$ and require a spectroscopic factor ($S = 1$) much larger than that required for the $^{16}O + {}^{28}Si$ data discussed earlier. However, all the energies shown on the right side of Fig. 9 have cross sections about 4 times lower than those on the left side and hence require $S = 0.5$ to reproduce their strength. For most of the angular distributions the phase is given reasonably well by the theoretical calculations, although there are a few cases (22.40, 27.30, and possibly 28.11 MeV) which would benefit by a shift of 1-2° (c.m.). While it seems possible that improvements to the phases can be achieved by parameter juggling, it is not obvious that the changes in the magnitudes of the experimental cross sections will be reproduced by the model. As one expects for a direct reaction theory, the magnitude of the DWBA cross section changes slowly with energy. Therefore, even though one can change the absolute magnitude of the calculations by means of variations in optical model or bound state parameters, it is difficult to imagine fitting such rapid cross section fluctuations short of employing different optical parameters at each energy - a tactic which seems unreasonable.

B. Other Data

Finally, we want to see what the model predicts for the $^{12}C + ^{28}Si$ system compared to existing data at high and low energies. In Fig. 10 we see that at E_{lab} = 29.00 MeV (the 20.3 MeV data in Fig. 9) the interference pattern does die out at angles forward of 70° c.m., but the amount of structure here is clearly exaggerated compared with that in the data. This may be due in part to our choice of optical potentials since, as shown in Fig. 11, at a somewhat higher energy of E_{lab} = 40.16 MeV the structure in the calculated angular distribution is in reasonable accord with published data.[16]) At still higher energy, E_{lab} = 49.3 MeV, the calculations (Fig. 12) are also consistent with measured data.[17])

V. SUMMARY

We have seen that elastic transfer calculations for $^{16}O + ^{28}Si$ appear capable of explaining the available data, at least qualitatively, with respect to the existence and phase of the back angle oscillations. However, it was found that some modification of the usual strongly absorbing optical potential E18 is required to raise the back angle elastic cross sections to a level which allows strong interference over a large angular range. For the $^{12}C + ^{28}Si$ system, which should be similar, the results are somewhat less encouraging. The available data fall into two groups requiring spectroscopic factors differing by a factor of 2. Here too, however, the phase of the back angle oscillations is given reasonably well by the calculations. Although more experimental data are clearly needed, it appears from the present

results that an exchange mechanism may play an important role in the anomalous back angle elastic scattering seen in the $^{16}O + ^{28}Si$ and $^{12}C + ^{28}Si$ systems.

VI. ACKNOWLEDGMENTS

I am grateful to P. Braun-Munzinger and R. DeVries for providing me with much of the data discussed here. The help of Elinor Potter in the preparation of the figures is also greatly appreciated.

This work was done with support from the U. S. Energy Research and Development Administration.

REFERENCES

1. J. G. Cramer, R. M. DeVries, D. A. Goldberg, M. S. Zisman, and C. F. Maguire, Phys. Rev. C 14, 2158 (1976).

2. D. S. Gale and J. S. Eck, Phys. Rev. C 7, 1950 (1973).

3. R. M. DeVries, D. A. Goldberg, J. Watson, M. S. Zisman, and J. G. Cramer, Phys. Rev. Lett. 39, 450 (1977).

4. R. M. DeVries, D. S. Shapira, N. Anantaraman, R. Cherry, M. R. Clover, and H. E. Gove, to be published.

5. P. Braun-Munzinger, G. M. Berkowitz, T. M. Cormier, C. M. Jachcinski, J. W. Harris, J. Barrette, and M. J. LeVine, Phys. Rev. Lett. 38, 944 (1977).

6. J. G. Cramer, J. C. Wiborg, Y-d Chan, K-L Liu, M. S. Zisman, B. D. Cuengco, W. L. Lynch, and R. J. Puigh, to be published.

7. W. N. Reisdorf, P. H. Lau, and R. Vandenbosch, Nucl. Phys. A235, 490 (1975).

8. C. K. Gelbke, R. Bock, and A. Richter, Phys. Rev. C 9, 852 (1974).

9. M. S. Zisman, R. Vandenbosch, and M. P. Webb, University of Washington Nuclear Physics Laboratory Annual Report, 1975 (unpublished), p. 122.

10. N. Austern, Direct Nuclear Reaction Theories, (Wiley-Interscience, New York, 1970), p. 354.

11. W. von Oertzen and H. G. Bohlen, Phys. Lett. 19C, 1 (1975).

12. Exact finite-range DWBA code LOLA, written by R. M. DeVries (unpublished); see also R. M. DeVries, Phys. Rev. C 8, 951 (1973).

13. W.F.W. Schneider, B. Kohlmeyer, F. Pühlhofer, and R. Bock, Nucl. Phys. A251, 331 (1975).

14. R. Stock, U. Jahnke, D. L. Hendrie, J. Mahoney, C. F. Maguire, W.F.W. Schneider, D. K. Scott, and C. Wolschin, Phys. Rev. C 14, 1824 (1976).

15. M. R. Clover, R. M. DeVries, R. Ost, N. Rust, R. N. Cherry, Jr., and H. E. Gove, Proc. of the International Conf. on Nuclear Structure, Tokyo, Sept. 5, 1977, p. 606.

16. L. Ray, G. Westfall, S.A.A. Zaidi, and W. R. Coker, Phys. Lett. 59B, 427 (1975).

17. I. Kohno, S. Nakajima, T. Tonuma, and M. Odera, Jour. Phys. Soc. Japan 30, 910 (1971).

Table I. Optical Model and Bound State Parameters

Set	V (MeV)	r_R [a] (fm)	a_R (fm)	W (MeV)	r_I [a] (fm)	a_I (fm)
			--- ^{16}O + ^{28}Si ---			
E18 [b]	10.0	1.35	0.618	23.4	1.23	0.552
O16C	10.0	1.36	0.57	3.6	1.38	0.30
Bound State [c]	-	1.25	0.75	-	-	-
			--- ^{12}C + ^{28}Si ---			
H12 [d]	10.0	1.326	0.617	30.3	1.162	0.609
C12F	30.1	1.36	0.44	67.3	1.28	0.32
Bound State [c]	-	1.35	0.80	-	-	-

[a] $R = r \times (A_p^{1/3} + A_t^{1/3})$

[b] Ref. 1

[c] Depth adjusted to match separation energy.

[d] Ref. 3

Figure Captions

Fig. 1 Kinematics of an elastic transfer reaction. The transfer reaction at angle $\pi-\theta$ is indistinguishable from the elastic scattering at angle θ.

Fig. 2 Formalism of elastic transfer calculations employing a full finite-range DWBA approach. The cross section is obtained by coherently adding the DWBA amplitude at angle $\pi-\theta$ to the elastic scattering amplitude at angle θ. Because of the symmetry of the reaction, only a single spectroscopic factor is required.

Fig. 3 Optical model and DWBA calculations for $^{16}O + ^{28}Si$ at $E_{lab} = 55$ MeV, compared with the data of Ref. 5. The DWBA calculations ($S = 0.3$) have been reflected about $\theta_{c.m.} = 90°$. Optical model and bound state parameters are given in Table I.

Fig. 4 Coherent addition of the cross sections shown in Fig. 3.

Fig. 5 Same as Fig. 3, but for optical potential 016C.

Fig. 6 Coherent addition of the cross sections shown in Fig. 5.

Fig. 7 Optical model and elastic transfer calculations for $^{16}O + ^{28}Si$ at $E_{lab} = 38$ MeV, compared with the data of Ref. 2.

Fig. 8 Optical model and elastic transfer calculations for $^{16}O + ^{28}Si$ at $E_{lab} = 81$ MeV, compared with the data of Ref. 1.

Fig. 9 Elastic transfer calculations for $^{12}C + ^{28}Si$ at the indicated center-of-mass energies, compared with the data of Ref. 15. Optical model and bound state parameters are listed in Table I. The data on the left side of the figure required $S = 1$ (solid curves) while those on the right side required $S = 0.5$ (dashed curves). See text.

Fig. 10 Optical model, DWBA, and elastic transfer calculations (using $S = 1$) for $^{12}C + ^{28}Si$ at $E_{lab} = 29.00$ MeV. The data are identical to the $E_{c.m.} = 20.30$ MeV data from Fig. 9.

Fig. 11 Optical model and elastic transfer calculations (using $S = 0.5$) for $^{12}C + ^{28}Si$ at $E_{lab} = 40.16$ MeV. The back angle data correspond to the $E_{c.m.} = 28.11$ MeV data from Fig. 9; the forward angle data are from Ref. 16.

Fig. 12 Optical model and elastic transfer calculations (using $S = 1$) for $^{12}C + ^{28}Si$ at $E_{lab} = 49.3$ MeV, compared with data from Ref. 17.

Elastic transfer mechanism

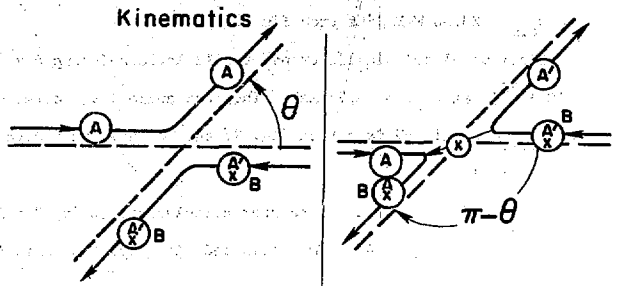

Scattering

$A + (A' + x)$
$\rightarrow A + (A' + x)$

Transfer

$A + (A' + x)$
$\rightarrow A' + (A + x)$

$A = A'$

Example:

$^{28}Si(^{16}O,^{16}O)^{28}Si$, $^{28}Si(^{16}O,^{28}Si)^{16}O$

XBL761-2003A

Figure 1

Elastic transfer

A. Elastic scattering amplitude

$$f_{el}(\theta) = \frac{i}{2k} \sum_{\ell} (2\ell + 1)(1 - e^{2i(\delta_\ell + \sigma_\ell)}) P_\ell (\cos\theta)$$

B. Transfer reaction amplitude

B (b,a) A

$$f_{DWBA}(\theta) \propto S_a^{1/2} S_B^{1/2} \int d\vec{r}_a \, d\vec{r}_b \, \chi_a^{(-)*}(\vec{r}_a) \, \psi_a^*(\vec{r}_{bx}) \, V_B(\vec{r}_{Ax}) \, \psi_B(\vec{r}_{Ax}) \, \chi_b^{(+)}(\vec{r}_b)$$

$$\propto S_a^{1/2} S_B^{1/2} \sum_{\ell} \beta_\ell P_\ell (\cos\theta)$$

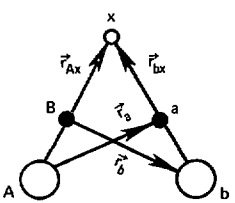

Spectroscopic amplitudes

$$S_a^{1/2} = S_B^{1/2} = S^{1/2} \propto \langle \psi_{^{28}Si} \mid \psi_{^{16}O} \otimes \psi_{^{12}C} \rangle$$

C. Cross section

$$\frac{d\sigma}{d\Omega} = | f_{el}(\theta) + e^{i\alpha} S \, f_{DWBA}(\pi - \theta) |^2$$

XBL 761 - 2001A

Figure 2

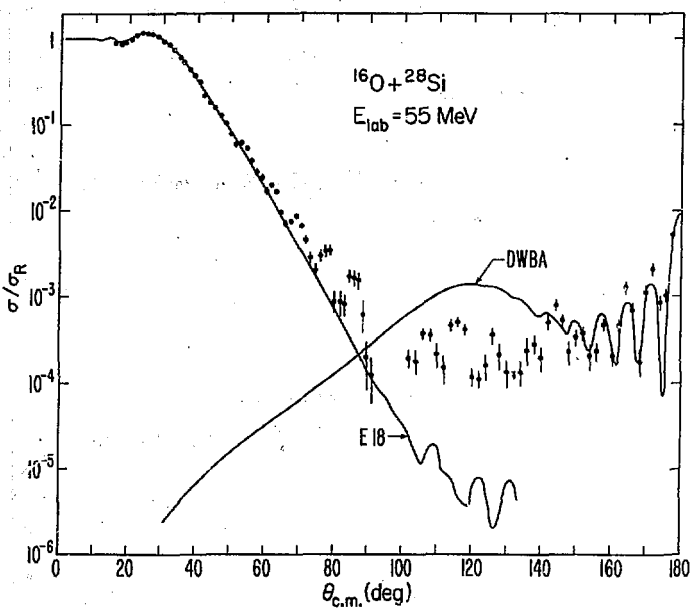
$^{16}O+^{28}Si$
E_{lab}=55 MeV
DWBA
E 18
σ/σ_R
$\theta_{c.m.}$(deg)
1
10^{-1}
10^{-2}
10^{-3}
10^{-4}
10^{-5}
10^{-6}
0
20
40
60
80
100
120
140
160
180
XBL 7710-2081

Figure 3

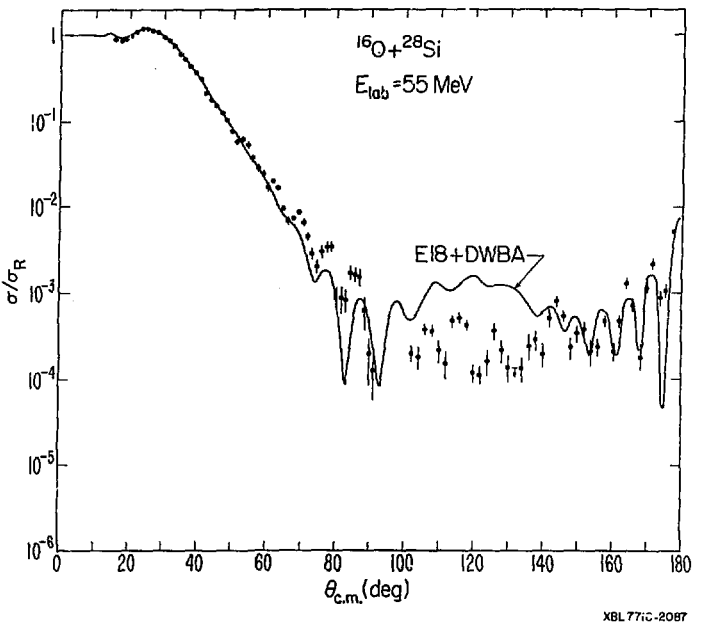
$^{16}O+^{28}Si$
E_{lab}=55 MeV
E18+DWBA
σ/σ_R
1
10^{-1}
10^{-2}
10^{-3}
10^{-4}
10^{-5}
10^{-6}
0
20
40
60
80
100
120
140
160
180
$\theta_{c.m.}$(deg)
XBL 7710-2087

Figure 4

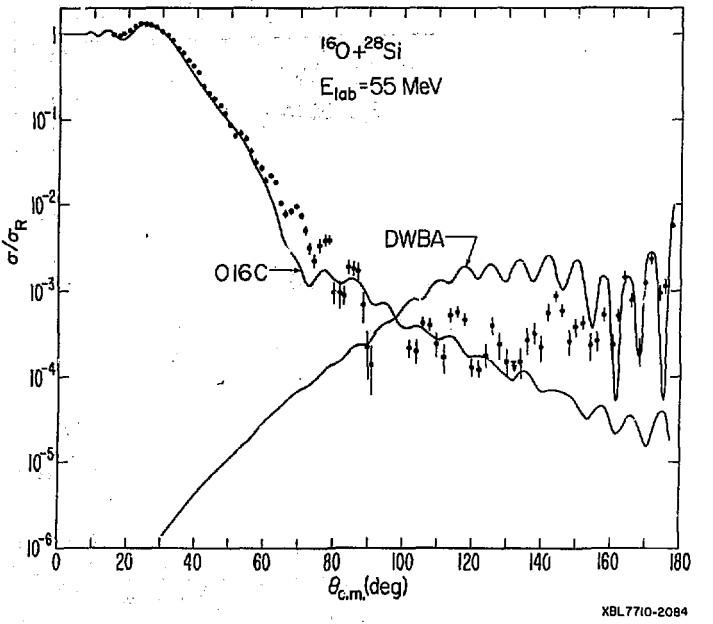
$^{16}O+^{28}Si$
E_{lab}=55 MeV
DWBA
O16C
σ/σ_R
1
10^{-1}
10^{-2}
10^{-3}
10^{-4}
10^{-5}
10^{-6}
0
20
40
60
80
100
120
140
160
180
$\theta_{c.m.}$(deg)
XBL7710-2084

Figure 5

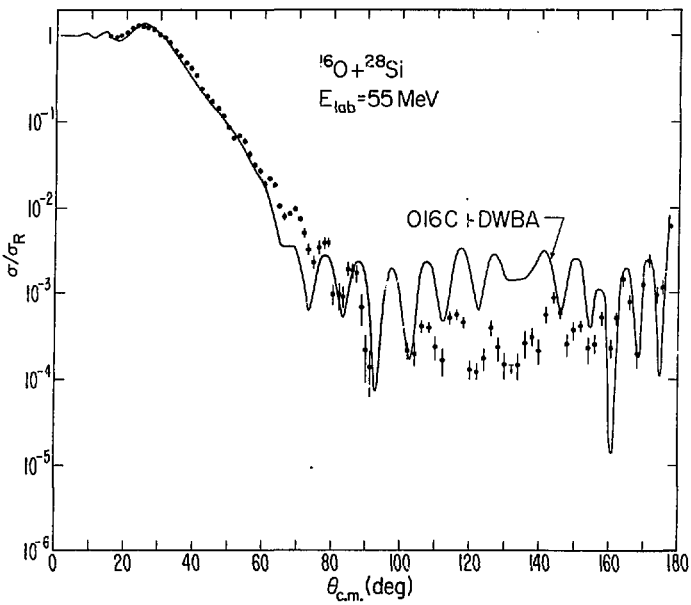
$^{16}O+^{28}Si$
E_{lab}=55 MeV
O16C + DWBA
σ/σ_R
1
10^{-1}
10^{-2}
10^{-3}
10^{-4}
10^{-5}
10^{-6}
0
20
40
60
80
100
120
140
160
180
$\theta_{c.m.}$(deg)
XBL7710-2088

Figure 6

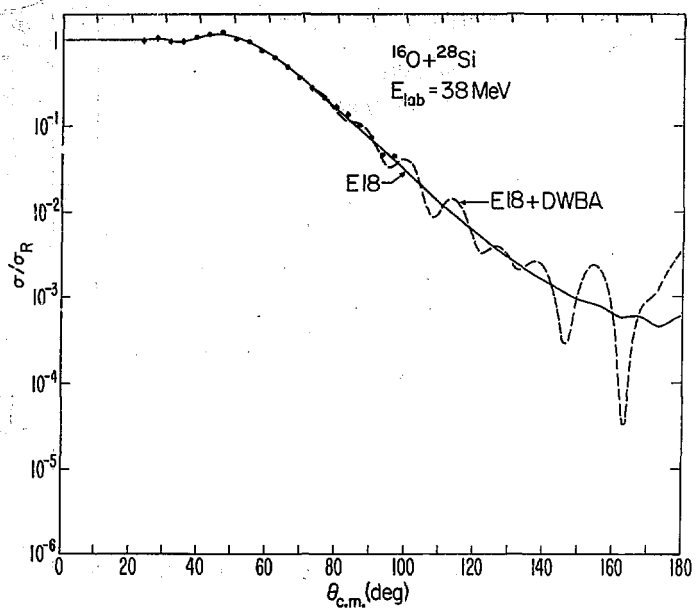

XBL 7710-2096

Figure 7

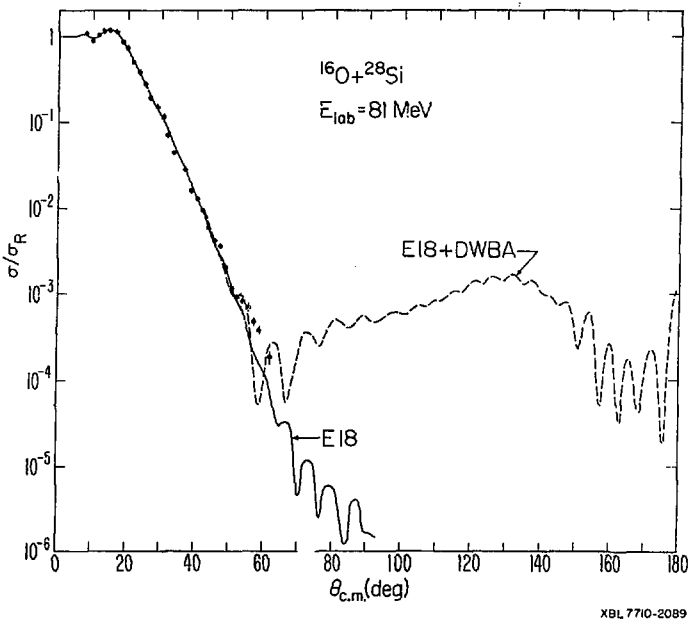
$^{16}O+^{28}Si$
E_{lab}=81 MeV
E18+DWBA
E18
σ/σ_R
$\theta_{c.m.}$(deg)
1
10^{-1}
10^{-2}
10^{-3}
10^{-4}
10^{-5}
10^{-6}
0
20
40
60
80
100
120
140
160
180
XBL 7710-2089

Figure 8

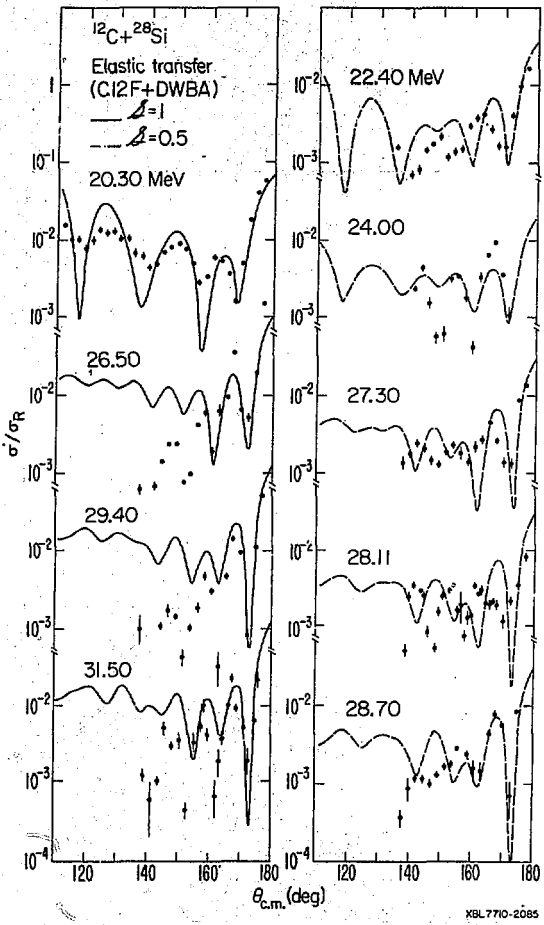
$^{12}C+^{28}Si$
Elastic transfer
(C12F+DWBA)
$\mathcal{J}$=1
$\mathcal{J}$=0.5
20.30 MeV
26.50
29.40
31.50
22.40 MeV
24.00
27.30
28.11
28.70
σ/σ_R
$\theta_{c.m.}$(deg)
XBL7710-2085

Figure 9

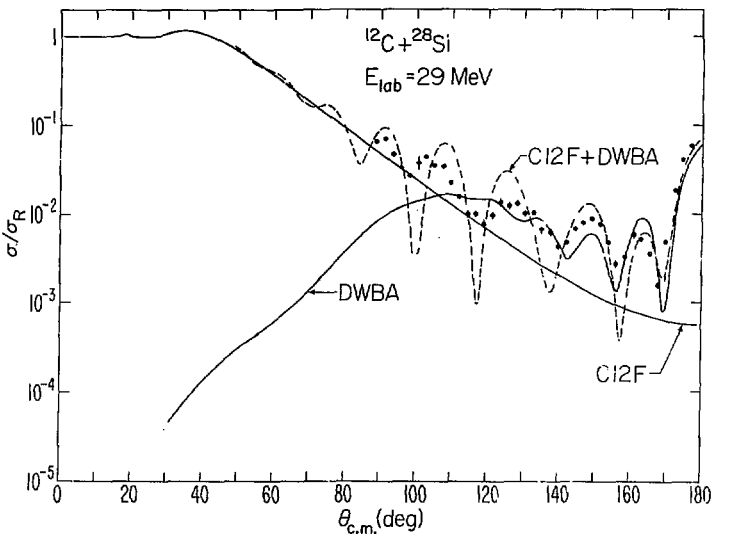
$^{12}C + ^{28}Si$
E_{lab} = 29 MeV
C12F+DWBA
DWBA
C12F
σ/σ_R
1
10^{-1}
10^{-2}
10^{-3}
10^{-4}
10^{-5}
0
20
40
60
80
100
120
140
160
180
$\theta_{c.m.}$(deg)
XBL 7710-2083

Figure 10

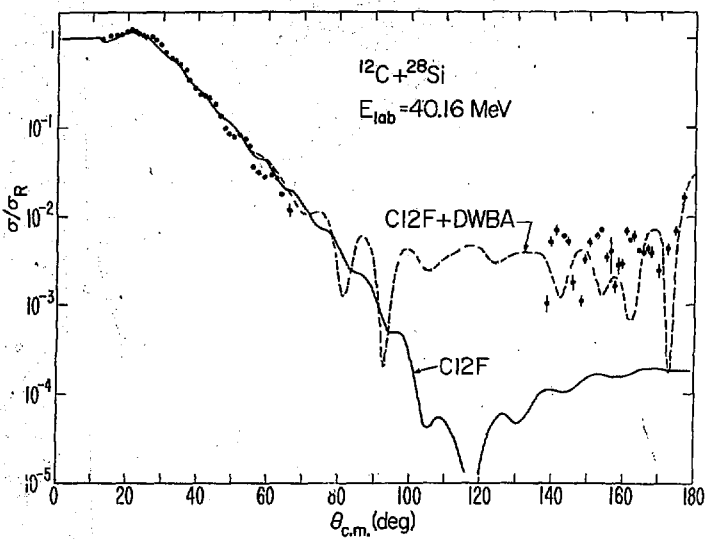
$^{12}C+^{28}Si$
E_{lab}=40.16 MeV
CI2F+DWBA
CI2F
σ/σ_R
1
10^{-1}
10^{-2}
10^{-3}
10^{-4}
10^{-5}
0
20
40
60
80
100
120
140
160
180
$\theta_{c.m.}$(deg)
XBL 7710-2082

Figure 11

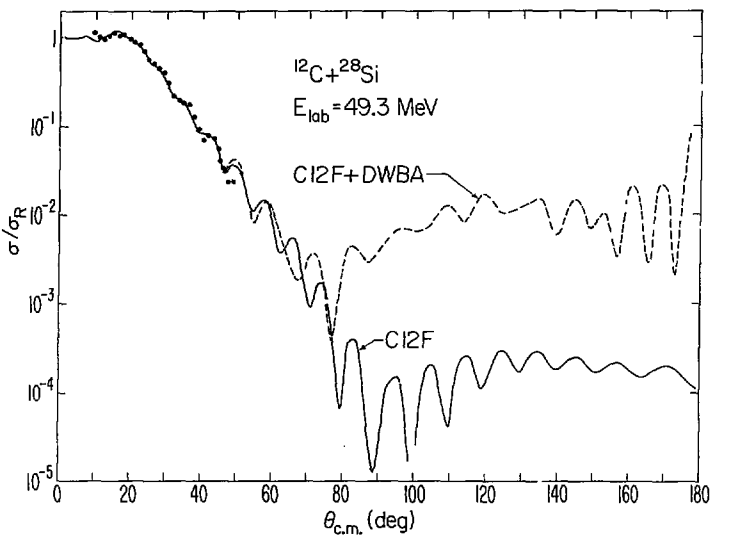
$^{12}C+^{28}Si$
E_{lab}=49.3 MeV
C12F+DWBA
C12F
σ/σ_R
1
10^{-1}
10^{-2}
10^{-3}
10^{-4}
10^{-5}
0
20
40
60
80
100
120
140
160
180
$\theta_{c.m.}$ (deg)
XBL7710-2080

Figure 12